A MODEL STUDY OF POWDER PARTICLE SIZE EFFECTS IN COLD SPRAY DEPOSITION

D. Helfritch and V. Champagne
U.S. Army Research Laboratory, Aberdeen Proving Ground, MD

ABSTRACT

The importance of high velocity for good particle deposition efficiency in the cold spray process is well known. Small particles achieve high velocities during nozzle acceleration, but also decelerate rapidly in the flow downstream of the bow shock wave. This study examines the effect of particle size on velocity and deposition efficiency in the cold spray process by means of flow modeling and gas-particle dynamics. Particle trajectories are modeled from the nozzle chamber to the impact with the substrate. Optimum particle size is identified for various particle characteristics and spray configurations.

LIST OF SYMBOLS

Parameter	Definition
A	area
C_D	drag coefficient
c_p	heat capacity
d	diameter
M	Mach number
m	mass
N_u	Nusselt number
p	pressure
P_r	Prandl number
R_e	Reynolds number
T	temperature
t	time
V	velocity
γ	specific heats ratio
ρ	density
σ	standard deviation
σ_μ	Ultimate tensile strength

1. INTRODUCTION

The U.S. Army utilizes metal coatings in many of its weapons systems for the strengthening or protection of vulnerable substrates. The quality of these coatings is characterized by the density of the metal coating and its ability to adhere to the substrate. Extremely dense and adherent metal coatings can be applied to surfaces by impacting metal particles onto the surface at supersonic velocities. This cold spray process is carried out at the U.S. Army Research Laboratory (ARL) in Aberdeen, MD.

Cold spray as a coating technology was initially developed in the mid-1980s at the Institute for Theoretical and Applied Mechanics of the Siberian Division of the Russian Academy of Science in Novosibirsk, Alkhimov et al., 1994, Tokarev, 1996. The Russian scientists successfully deposited a wide range of pure metals, metallic alloys, polymers, and composites onto a variety of substrate materials, and they demonstrated that very high coating deposition rates are attainable using the cold spray process. Currently, a variety of cold spray research is being conducted at institutions in the United States, Russia, Germany, and Japan, Papyrin, 2001.

The ARL system accelerates micron-sized particles to high velocities by entraining the particles in the flow of a supersonic nozzle. This system is shown in Fig. 1, Assadi et al., 2003. High velocity is necessary for an optimal particle deposition and coating density, and several parameters, including gas conditions, particle characteristics, and nozzle geometry, affect the particle velocity. This work examines the effects of these parameters on coating characteristics.

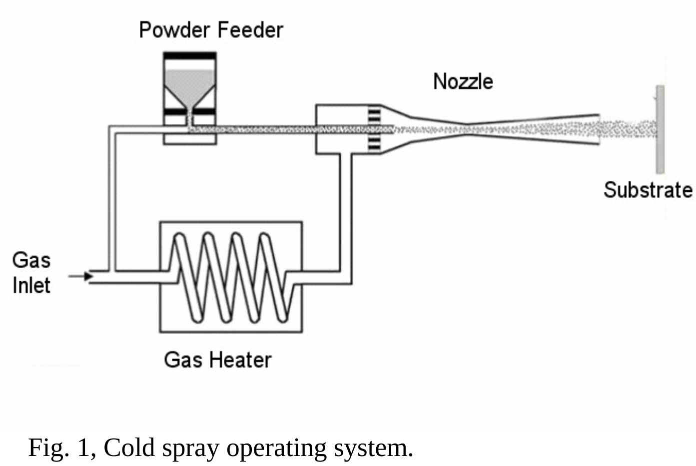

Fig. 1, Cold spray operating system.

Report Documentation Page

Form Approved
OMB No. 0704-0188

1. REPORT DATE **DEC 2008**	2. REPORT TYPE **N/A**	3. DATES COVERED -

4. TITLE AND SUBTITLE **A Model Study Of Powder Particle Size Effects In Cold Spray Deposition**	5a. CONTRACT NUMBER 5b. GRANT NUMBER 5c. PROGRAM ELEMENT NUMBER
6. AUTHOR(S)	5d. PROJECT NUMBER 5e. TASK NUMBER 5f. WORK UNIT NUMBER
7. PERFORMING ORGANIZATION NAME(S) AND ADDRESS(ES) **U.S. Army Research Laboratory, Aberdeen Proving Ground, MD**	8. PERFORMING ORGANIZATION REPORT NUMBER
9. SPONSORING/MONITORING AGENCY NAME(S) AND ADDRESS(ES)	10. SPONSOR/MONITOR'S ACRONYM(S) 11. SPONSOR/MONITOR'S REPORT NUMBER(S)

12. DISTRIBUTION/AVAILABILITY STATEMENT
Approved for public release, distribution unlimited

13. SUPPLEMENTARY NOTES
See also ADM002187. Proceedings of the Army Science Conference (26th) Held in Orlando, Florida on 1-4 December 2008, The original document contains color images.

14. ABSTRACT

15. SUBJECT TERMS

16. SECURITY CLASSIFICATION OF:			17. LIMITATION OF ABSTRACT	18. NUMBER OF PAGES	19a. NAME OF RESPONSIBLE PERSON
a. REPORT **unclassified**	b. ABSTRACT **unclassified**	c. THIS PAGE **unclassified**	**SAR**	**5**	

Standard Form 298 (Rev. 8-98)
Prescribed by ANSI Std Z39-18

2. MODEL STRUCTURE

The modeling of deposition efficiency, or particles building up over previously deposited particles, can be broken down into three tasks:

1. The gas flow and temperature in the nozzle are calculated by means of isentropic (frictionless) gas dynamic principles.
2. Drag and heat transfer coefficients from solid rocket analyses are used to iteratively calculate particle velocity and temperature through the nozzle.
3. An empirical relationship between the particle velocity and particle material characteristics is used to calculate the deposition efficiency or the percent of incoming particles that adhere and form the coating.

2.1 Gas Flow

The gas flow model uses isentropic relationships and linear nozzle geometry. The assumptions for the calculation are as follows:

- The gas obeys the perfect gas law.
- There is no friction impeding the gas flow.
- The gas flow is adiabatic, i.e., no heat loss occurs to the surroundings.
- Steady-state conditions exist.
- Expansion of the gas occurs in a uniform manner without shock or discontinuities.
- Flow through the nozzle is one-dimensional; hence, the flow velocity, pressure, and density are uniform across any cross section normal to the nozzle axis.
- Particles do not influence gas conditions.

Under these conditions, the relationship, Shapiro, 1953, between the nozzle area, A, and the Mach number is given by Equation 1, where γ is the ratio of gas specific heats (C_p/C_v):

$$\frac{A_1}{A_2} = \frac{M_2}{M_1}\left\{\frac{1+[(\gamma-1)/2]M_1^2}{1+[(\gamma-1)/2]M_2^2}\right\}^{\frac{(\gamma+1)}{2(\gamma-1)}} \qquad \text{(Eq 1)}$$

The simple, conical nozzle geometry shown in Fig. 2 is assumed. A small initial subsonic Mach number and initial (stagnation) values of pressure and temperature are assigned at the converging section of the nozzle. The Mach number is then iteratively increased, while gas characteristics are calculated for each point through the isentropic relationships of Equations 2 and 3. Linear progression along the nozzle axis is calculated from the area change given by Equation 1 and the assumed nozzle geometry.

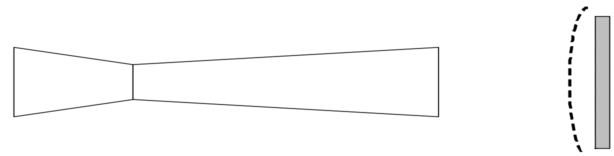

Fig. 2, Nozzle-shock wave-substrate geometry.

$$\frac{T_0}{T} = 1+\left(\frac{\gamma-1}{2}\right)M^2 \qquad \text{(Eq 2)}$$

$$\frac{p_0}{p} = \left[1+\left(\frac{\gamma-1}{2}\right)M^2\right]^{\frac{\gamma}{\gamma-1}} \qquad \text{(Eq 3)}$$

The flow between the nozzle exit and the shock wave upstream of the substrate is assumed to be constant, and equal to the conditions at the nozzle exit. The stand-off position of the shock wave relative to the substrate is given by Billig's approximation, Billig, 1967, as:

$$\Delta = 0.143 d_e\left[\exp\left(3.24/M_e^{\,2}\right)\right] \qquad \text{(Eq 4)}$$

where d_e equals the nozzle exit diameter, and M_e is the Mach number at the nozzle exit.

The Mach number immediately behind the shock wave is given by the normal shock relationship:

$$M^2 = \frac{\left[M_e^{\,2} + \dfrac{2}{\gamma-1}\right]}{\left[\left(\dfrac{2\gamma}{\gamma-1}\right)M_e^{\,2} - 1\right]} \qquad \text{(Eq 5)}$$

Downstream of the shock wave, the Mach number is assumed to linearly decrease from the value given by Equation 5 to zero at the substrate surface.

2.2 Particle Motion

Once the gas conditions and velocity are characterized, the particle velocity is iteratively calculated from the nozzle entrance to the substrate through the use of a solid rocket nozzle particle drag relationship. This relationship predicts the accelerating force on the particle:

$$m\frac{dV_p}{dt} = C_D(\pi/8)\rho_g d^2 (V_g - V_p)^2 \qquad \text{(Eq 6)}$$

V_p and V_g are particle and gas velocities, m is the particle mass, ρ_g is the gas density, and d is the particle diameter. Carlson and Hoglund, 1964, correct the simple Stokes drag law relationship for inertial, compressibility, and rarefaction effects through the empirical relationship of Equation 7:

$$C_D = \frac{24}{R_e}\left[\frac{\left(1+0.15R_e^{0.687}\right)\left(1+e^{-0.427/M_p^{4.63}+3.0/R_e^{0.88}}\right)}{1+\left(M_p/R_e\right)\left(3.82+1.28e^{-1.25R_e/M_p}\right)}\right] \qquad \text{(Eq7)}$$

where M_p is the Mach number of the gas-particle velocity difference and R_e is the gas-particle Reynolds number. Particle temperature is subsequently calculated through the application of the gas-particle heat transfer relationship for forced convection, given by Equation 8:

$$c_p\frac{dT_p}{dt} = \left(N_u k/d_p\right)\left(A_p/m\right)\left(T_g - T_p\right) \qquad \text{(Eq 8)}$$

where c_p is the particle heat capacity, T_p and T_g are the particle and gas temperatures, N_u is the Nusselt number, k is the gas conductivity, and A_p is the particle surface area. Ranz and Marshall, 1952, show that the Nusselt number for this situation is given by

$$N_u = 2.0 + R_e^{0.5}P_r^{0.33} \qquad \text{(Eq 9)}$$

where P_r is the Prandl number.

2.3 Deposition Efficiency

The ability to predict the deposition efficiency allows one to choose gas and particle parameters that will yield a good deposition efficiency and reduce the operating time and wasted powder. An empirical relationship between particle parameters and the critical velocity needed for a particle to stick to a previously deposited layer and the gas dynamic velocity model shown above are used to predict the deposition efficiency. The empirical relationship for the particle critical velocity, V_c, is given by Assadi et al. [4] as:

$$V_c = 667 - 14\rho_p + 0.08T_m + 0.1\sigma_\mu - 0.4T_e \qquad \text{(Eq 10)}$$

where ρ_p = particle density, T_m = particle melting point, σ_μ = particle UTS, and T_e = particle exit temperature.

The critical velocity as determined by Equation 10 and the particle velocities as a function of diameter then allow an identification of the particle diameters that can achieve this velocity. It will be shown that the diameter of particles that exceed critical velocity are limited at both the small end and the large end of a range of diameters.

The powders employed in cold spray are not of uniform diameter but are characterized by a distribution of particle diameters, and the distribution is defined as normal. Deposition efficiency is calculated as the percent of particles having a smaller diameter than the largest particle diameter achieving the critical velocity minus the percent of particles having a smaller diameter than the smallest particle that can achieve the critical velocity. For a normal distribution, Equation 11 defines the mass percent of particles having a smaller diameter than the particle diameter, d_p, where MMD is the mass mean diameter of the feed stock powder and σ is the geometric standard deviation of the distribution. Once the smallest and the largest particles that reach the critical velocity are determined, the percent of particles smaller than the smallest particle achieving the critical velocity is subtracted from the percent of particles smaller than the largest particle. The result of this subtraction is the deposition efficiency:

$$\% = \left(\frac{100}{2}\right)\left[1 + erf\left(\frac{d_p - MMD}{\sigma\sqrt{2}}\right)\right] \qquad \text{(Eq 11)}$$

3. CALCULATIONS AND DISCUSSION

Nitrogen gas is used for these calculations. The gas stagnation (chamber) pressure and temperature are 2.76 MPa and 673 K, unless otherwise noted. The initial particle temperature is 293 K. The nozzle length is 10 cm, its throat diameter is 2 mm, and its area ratio is 4.

Spherical particles are assumed. The mass ratio of particles to gas in typical cold spray operation is less than 0.05; therefore, it is assumed that the presence of particles does not affect the gas flow and that no particle-to-particle contact occurs. An individual calculation applies to a single particle of a given diameter. Particle size effects are determined by multiple calculations for various particle diameters.

Figure 3 shows a gas-particle calculation for 3 µm copper particles. Nitrogen gas, initially at 2.76 MPa and 673 K, is the main gas. The gas converts temperature and pressure into velocity as it is expanded in the converging-diverging nozzle. The gas attains Mach 1 at the throat and is about Mach 3 at the nozzle exit. Particle velocity is related to the gas velocity through the drag relationship, Equation 6. A gas exit velocity of 950 m/s and a particle exit velocity of 850 m/s are seen for this case. Particle temperature is related to the gas temperature through convective heat transfer, Equation 8. The particles are seen to heat up when they are cooler than the gas and begin to cool down after the gas has expanded to temperatures lower than that of the particles. The gas velocity is constant between the nozzle exit and the shock wave, while particle velocity increases somewhat.

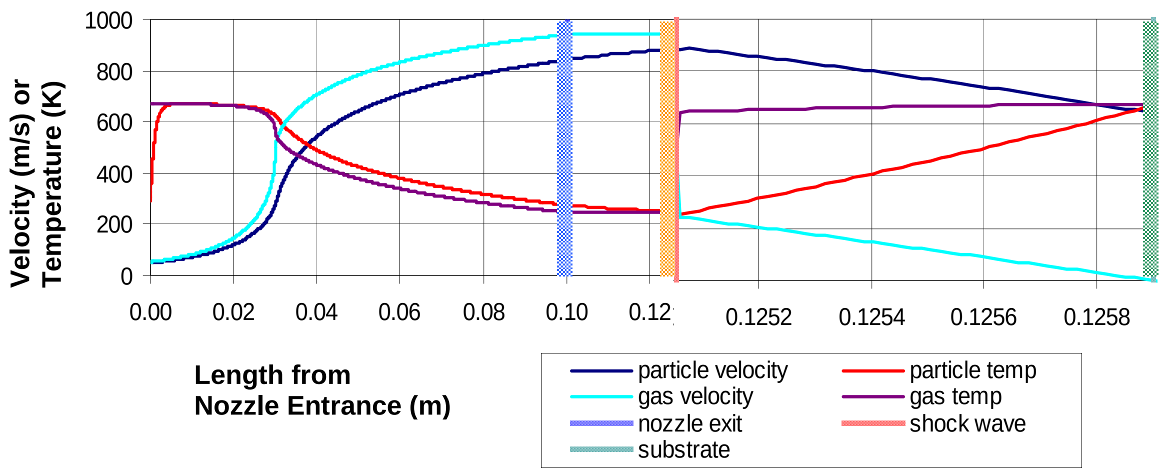

Fig. 3, Gas-particle nozzle flow impacting a substrate (note scale change).

The axis scale of the zone downstream of the shock wave is expanded in order to observe parameters in this length of less than 1 mm. As for all supersonic flow impacting an object, the flow correction is made by a shock wave which instantly reduces gas velocity to subsonic and increases gas pressure and temperature. Particle velocity and temperature are not instantly affected by the shock wave, but continue to be affected by gas velocity and temperature through drag and heat transfer, (equations 6 and 8). Gas velocity decreases linearly downstream of the shock to zero at the substrate surface. Accordingly, particle velocity also decreases and is at a value lower than that at the nozzle exit when it strikes the substrate. Thus the use of nozzle exit velocities for deposition estimates can result in an incorrectly high deposition efficiency.

Figure 4 shows how the particle impact velocity is affected by particle size for three values of particle density.
The figure clearly shows that an optimum particle size exists for each density. Larger particles are relatively unaffected by the shock and achieve velocities consistent with the expectation that lighter (less dense) particles have a higher velocity. The reverse is true for smaller particles, where lighter particles are decelerated most severely downstream of the shock wave. Large particles exit the nozzle at a lower velocity, but maintain this velocity past the shock wave. Thus there exists an optimum particle size which has a relatively high exit velocity but is relatively unaffected by the subsonic gas flow downstream of the shock.

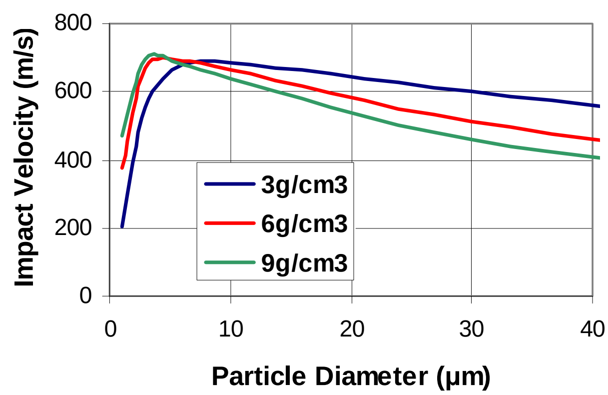

Fig. 4, Impact velocity as a function of the particle size for three particle densities.

Figure 5 results when the critical velocity for particle deposition (Equation 10) is included with the results of Fig. 4 for copper particles (9 g/cm^3). Particles between 1.5 and 15 µm are seen to exceed the critical velocity and are therefore deposited. Particles smaller than 1.5 µm and larger than 15 µm do not deposit. Thus for the distribution of particles within this feed stock powder, the deposition efficiency would be the weight percent of particles between 1.5 and 15 µm.

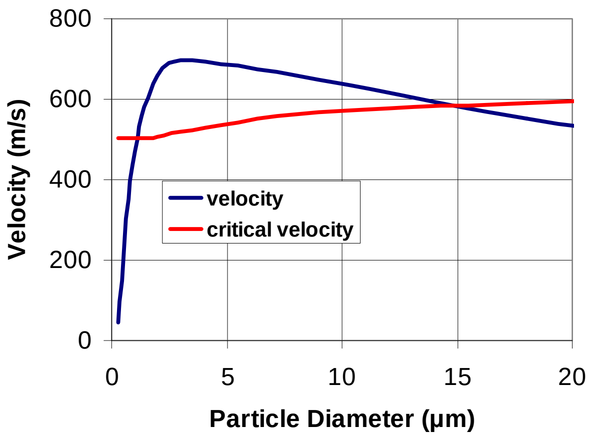

Fig. 5, Impact and critical velocities as a function of the particle size.

For comparison, the deposition efficiency is calculated for the case when a shock wave is present, as well as when no shock is present and particles impact at nozzle exit velocity. Deposition efficiency is calculated as a function of the mass mean diameter of copper powder having a normal distribution and a standard deviation of 4. Figure 6 shows the results of these calculations. The figure shows that the presence of the shock wave has essentially no effect when spraying powders with distributions of mass mean diameter greater than 10 µm; however, shock–induced effects become large for smaller MMDs. This occurs because large particles are not affected by the reduced gas velocity during the short period of time between the shock and the substrate, while small particles are affected.

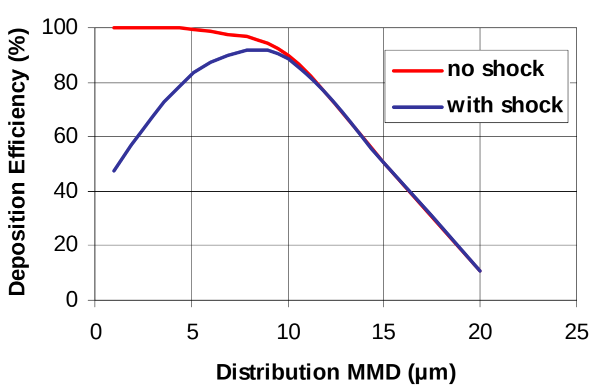

*F*ig. 6, Deposition efficiency as a function of the particle distribution mass mean diameter.

CONCLUSIONS

Particle deposition and consolidation by cold spray has been modeled through the application of conventional rocket nozzle flow equations and the application of an empirical materials-driven impact relationship. Particle velocities and temperatures were predicted at the nozzle exit, downstream of the bow shock and at the substrate surface. These conditions were subsequently used to predict the deposition efficiency.

It has often been thought that the smallest particles attain highest velocities in the cold spray process, thus achieving good deposition efficiency. While it is true that small particles exit the nozzle at high velocity, their velocity at impact can be significantly lower. Modeling efforts showed that the low gas velocity following the bow shock wave decreases particle velocities, especially for the smallest particles. It was shown that impact velocity increases as the particle diameter decreases until a diameter of 4 to 8 µm is reached. Impact velocity then decreases as the particle diameter is further reduced. This effect can reduce the deposition efficiency from 90% at a MMD of 8 µm to 50% at 2 µm. These observations have been qualitatively known in the cold spray community but quantitative guidelines were not well established. The modeling effort presented here gives the ability to anticipate coating results based upon the spray parameters and material characteristics, thus eliminating trial and error attempts at creating acceptable coatings.

REFERENCES

Alkhimov, A.P., et al., 1994: Gas Dynamic Spraying Method for Applying a Coating, US Patent 5,302,414.

Assadi, H., et al., 2003: Bonding Mechanism in Cold Gas Spraying, *Acta Materialia*, Vol. 51, pp.4379–4394.

Billig, F.S., 1967: Shock-Wave Shapes around Spherical and Cylindrical-Nosed Bodies, J. *Spacecraft*, Vol. 4(No. 5), pp. 822 - 823.

Carlson, D. and Hoglund, R., 1964: Particle Drag and Heat Transfer in Rocket Nozzles, *AIAA Journal*, Vol 2 (No. 11), pp. 1980 -1984.

Papyrin, A., 2001: Cold Spray Technology, *Adv. Mater. Process*, p. 49–51.

Ranz, W.E. and Marshall, W.R., 1952: Evaporation from Drops, *Chem. Eng. Prog*.,Vol 48, pp. 141-146.

Shapiro, A., 1953: *The Dynamics and Thermodynamics of Compressible Fluid Flow*, Roland Press, New York.

Tokarev, A.O., 1996: Structure of Aluminum Powder Coatings Prepared by Cold Gas Dynamic Spraying, *Met. Sci. Heat Treat*, Vol. 35, p. 136.